

The Interstellar Medium: The Key Component in Galactic Evolution and Modern Cosmology

Carl Heiles¹, Di Li^{2,3,4}, Naomi McClure-Griffiths⁵, Lei Qian^{2,3}, Shu Liu^{2,3}

¹ Department of Astronomy, University of California, Berkeley, 601 Campbell Hall 3411, Berkeley, CA 94720-3411; heiles@astro.berkeley.edu

² National Astronomical Observatories, Chinese Academy of Sciences, Beijing 100101, China

³ Key Laboratory of FAST, National Astronomical Observatories, Chinese Academy of Sciences, Beijing 100101, China

⁴ University of Chinese Academy of Sciences, Beijing 100049, China

⁵ Research School for Astronomy & Astrophysics, Australian National University, Canberra, ACT 2611, Australia

Received 20XX Month Day; accepted 20XX Month Day

Abstract The gases of the interstellar medium (ISM) possess orders of magnitude more mass than those of all the stars combined and are thus the prime component of the baryonic universe. With L-band surface sensitivity even better than the planned phase one Square-Kilometer-Array (SKA1), the Five-hundred-meter Aperture Spherical radio Telescope (FAST) promises unprecedented insights into two of the primary components of ISM, namely, the atomic hydrogen (HI) and the hydroxyl molecule (OH). We discuss here the evolving landscape of our understanding of ISM, particularly, its complex phases, the magnetic fields within, the so-called dark molecular gas (DMG), high velocity clouds, and the connection between local and distant ISM. We lay out, in broad strokes, several expected FAST projects, including an all northern-sky high-resolution HI survey (22,000 deg², 3' FWHM beam, 0.2 km/s), targeted OH mapping, searching for absorption or masing signals, and etc. Currently under commissioning, the commensal observing mode of FAST will be capable of simultaneously obtaining HI and pulsar data streams, making large-scale surveys in both science areas more efficient.

Key words: ISM: atoms — ISM: individual (hydrogen) — ISM: molecules — ISM: evolution — surveys

1 INTRODUCTION: COSMOLOGICAL EVOLUTION AND THE INTERSTELLAR GAS

Our knowledge of how the Universe has evolved is completely different today from what it was two decades ago. From cosmology and extragalactic astronomy we now have a theory based on cold, dark matter, called DM, that explains with reasonable accuracy the Universe from its first few minutes, through the formation of the first galaxies, to the present era where clusters of galaxies dominate the Universe (e.g. [Sommer-Larsen et al. 2003](#), [Komatsu et al. 2009](#)). This theory has been applied in simulations of the Universe that show streams of gas coming together to form the essential building blocks of the Universe, galaxies. These galaxies in turn come alive through bursts of star formation, lose gas to their surroundings and simultaneously accrete new gas to continue their ravenous star formation habit.

Eventually after billions of years when their gas supplies run out they cease their star formation, living on perpetually as increasingly red objects filled with low-mass stars.

Thus, the evolution of galaxies is inextricably linked to the interstellar gas, and this is where the models break down. We know that the life cycle of the Milky Way and most galaxies involves a constant process of stars ejecting matter and energy into the interstellar mix, from which new stars then condense, continuing the cycle. For this part of the theory observational or empirical assumptions are inserted, rather than the detailed physics that drives the rest of the models. If we are to understand how galaxies evolve, we must first understand the physics of their evolution in environments we can observe in detail. Our own Galaxy, the Milky Way, provides us with the closest laboratory for studying the evolution of gas in galaxies, including how galaxies acquire fresh gas to fuel their continuing star formation, how they circulate gas and how they turn warm, diffuse gas into molecular gas and ultimately, stars. The Milky Way is a very complex ecosystem. Just as ecosystems on Earth involve many elements linked together by a common source of nutrients and energy flow, the Milky Way ecosystem consists of stars fuelled by a shared pool of gas in the interstellar medium (ISM) and energy that flows back and forth between the stars, the ISM and out of the Galactic disk.

We need to understand the details of these gasdynamical processes that lie at the very heart of the astrophysics. How, exactly, do galaxies form stars, acquire fresh gas, recycle their own gas to form new stars, respond to and dissipate the large-scale energy inputs from supernova and galactic shocks on scales from galactic to sub-parsec. These overarching processes are, in turn, affected by the detailed physical conditions. In particular, these include pressure, temperature, ionization state, magnetic field, degree of turbulence, chemical composition, morphology, and the effects of gravity.

2 INTERSTELLAR MATTER IN THE MILKY WAY

Once thought to be a simple, quiescent medium, the ISM is now known to include a number of diverse constituents, which exhibit temperatures and densities that range over six orders of magnitude. The ISM is composed of gas in all its phases (ionized, atomic and molecular), dust, high energy particles and magnetic fields, all of which interact with the stars and gravitational potential of a galaxy to produce an extraordinary, dynamic medium.

2.1 Phases of the ISM

2.1.1 *The Classical Five Phases*

In the Solar vicinity, astronomers generally recognize five phases of interstellar gas: dense molecular clouds, which are traced by CO line emission; the atomic Cold and Warm Neutral Media (CNM and WNM), traced by the 21-cm line; the Warm Ionized Medium (WIM), traced by pulsar dispersion and $H\alpha$ emission; and the Hot Ionized Medium (HIM), traced by X-ray emission. The atomic and molecular phases have comparable mass (the molecular phase rises and dominates toward the Galactic interior's 'Great Molecular Ring') and the WIM is somewhat less.

2.1.2 *Dark Gas: The Sixth Phase*

However, there lurks a sixth phase: Dark Molecular Gas, in which Hydrogen is molecular but the usual H_2 tracer, CO emission, is absent. Dark Molecular Gas was discovered (we believe) when [Dickey et al. \(1981\)](#) found OH in absorption against high Galactic latitude continuum sources. Important and extensive confirmatory absorption measurements by [Liszt & Lucas \(1996\)](#) and [Lucas & Liszt \(1996\)](#) found that OH and HCO^+ are commonly observed against such sources. These two molecules are much more easily seen in absorption than emission because their excitation temperatures T_x are low. In the relatively thin clouds where they reside the collisional excitation rates are small so that $T_x \ll T_k$, which was borne out by our analysis ([Li et al. 2018b](#), also Sec. 2.3 in this work) of the Millennium survey data ([Heiles & Troland 2003](#)).

Historically, molecular lines were seen mainly in emission towards the standard dense molecular clouds, and CO was emphasized to the extent that its presence *defined* molecular gas. While most astronomers remain unaware that Dark Molecular Gas is so prominent, a few courageous radio astronomers have pursued Dark Molecular Gas through spectroscopy. Liszt and his collaborators, primarily Lucas and Pety, have observed absorption and emission lines of OH, HCO⁺, and CO to establish abundance ratios, and they have mapped CO in the Dark Molecular Gas regions; this work currently culminates in the comprehensive presentation of Liszt & Pety (2012), who show CO emission maps together with CO, HCO⁺, and OH absorption spectra for 11 continuum sources. Cotten et al. (2012) and Cotten & Magnani (2013) mapped CH and OH around the dense molecular cloud MBM40. Allen et al. (2012, 2015) found extensive OH emission in their map; at most positions, CO emission was absent. Studies of individual clouds, e.g. the Taurus Molecular Cloud (TMC, Xu et al. 2016, Xu & Li 2016), also tend to find substantial CO-dark molecular gas. Quite generally, observers find the mass of Dark Molecular Gas to be comparable to that of the CO-bright molecular gas.

It's not just radio astronomers! Grenier et al. (2005) used the Energetic Gamma Ray Experiment Telescope (EGRET) to map the diffuse Galactic gamma rays produced by the interaction of cosmic rays with H-nuclei. The gamma-ray intensity is proportional to the total H-nuclei column density, whether in atomic or molecular form; comparing with CO emission unveils the Dark Molecular Gas (DMG). They find that the Dark Molecular Gas is very common throughout the Galaxy, even in the interior. It surrounds all the nearby CO clouds and bridges the dense cores with the broader atomic clouds, thus providing a key link in the evolution of interstellar clouds. The general trend of the fraction of the gamma-ray identified DMG are found to follow those of simple hydrides (Remy et al. 2018). As they conclude, "The relation between the masses in the molecular, dark, and atomic phases in the local clouds implies a dark gas mass in the Milky Way comparable to the molecular one."

2.2 The CNM

2.2.1 The CNM and Its Relation to Dark Molecular Gas

It seems almost certain that Dark Molecular gas is a transition state between the CNM and classical molecular clouds. This emphasizes the importance of studying the CNM together with the prime DMG tracers, OH and HCO⁺. They will tell us where the formation of molecules is initiated, and the detailed comparison of the atomic and molecular spectral lines will provide the temperature and density. Moreover, we expect the details of the DMG transition region to depend not only on physical conditions but also cloud *morphology*. Morphology determines whether UV photons can penetrate to destroy molecules via photodissociation or photoionization. It seems to us very unlikely that one can understand the transition between atomic and molecular gas without understanding the effect of UV photons, and thus cloud morphology. Moreover, there are hints that cloud morphology is affected by the magnetic field; after all, magnetic forces are one of the important forces on the ISM (the others being turbulent pressure, cosmic ray pressure (coupled to the gas by the magnetic field), thermal pressure, and gravity).

2.2.2 CNM: Physical conditions

Our current knowledge of physical conditions and morphology in the CNM depends overwhelmingly on results from the Millennium survey of Heiles & Troland (2005) (HT), who used Arecibo with long integration times suitable for detecting Zeeman splitting. For the HI line in absorption, HT derived column densities, temperatures, turbulent Mach number, and magnetic fields. HI CNM Column densities are usually below 10^{20} cm^{-2} with a median value $N(HI)_{20} \sim 0.5$. The median spin temperature $T_s \sim 50 \text{ K}$ and the median turbulent Mach number ~ 3.7 . The median magnetic field $\sim 6 \mu\text{G}$ (Heiles & Troland 2005); this is a statistical result and individual detections are too sparse to make a meaningful histogram.

2.2.3 CNM: Morphology

Regarding morphology, Heiles & Troland (2003), in their Section 8, present one of the few discussions of 3-d CNM morphology. By assuming reasonable values for the thermal gas pressure and comparing observed column densities, shapes and angular sizes as seen on the sky, they find that interstellar CNM structures cannot be characterized as isotropic. The major argument is that a reasonable interstellar pressure, combined with the measured kinetic temperature, determines the volume density; this, combined with the observed column density, determines the thickness of the cloud along the line of sight. This dimension is almost always much smaller than the linear sizes inferred from the angular sizes seen on the sky. Heiles & Troland (2003) characterize the typical structures as ‘blobby sheets’, and this applies for angular scales of arcseconds to degrees. An alternative, which they did not discuss, is that the structures are more spherical, but spongelike inside. (If they are spongelike, what fills the holes?)

Apart from this general argument, only a very few individual interstellar structures have been characterized morphologically. One important reason for the small numbers is the difficulty of mapping the 21-cm line with simultaneously high brightness temperature sensitivity and high angular resolution. Single dishes have high sensitivity and low resolution, while interferometers have high resolution but low sensitivity. The GALFA 21-cm line survey (Peek et al. 2011b), which is a fully-sampled survey of the entire Arecibo sky (declination 0° to 39° , about 1/3 of the entire sky) provides the best of both worlds, with angular resolution 3.4 arcminutes and sensitivity 0.1 K. FAST will do even better!

The most spectacular result is the ‘Local Leo Cold Cloud’ (LLCC: Peek et al. 2011a, Meyer et al. 2012), which we characterize as a remarkably thin sheet. Figure 1 images the LLCC, with color indicating the residual radial velocity after subtracting a clear velocity gradient along the length of the cloud, which amounts to about 1 km s^{-1} . The cloud temperature, in some places less than 20 K, is measured at a few positions both by emission/absorption of the 21-cm line and by optical/UV spectroscopy. The UV absorption lines of CI provide the interstellar pressure, $P/k \sim 60000 \text{ cm}^{-3} \text{ K}$, which exceeds the typical interstellar pressure by well over an order of magnitude. The pressure and temperature provide the density, $n(HI) \sim 3000 \text{ cm}^{-3}$; the observed column density, $N(HI)_{20} \sim 0.04$, provides the thickness along the line of sight—about 200 AU. The cloud distance lies between 11 and 24 pc; this close distance, combined with the absorption of diffuse X-rays mapped by ROSAT, confirms the absence of hot gas inside the Local Bubble. With the LLCC’s angular dimension of several degrees, its extent on the plane-of-the-sky is about 1 pc. The aspect ratio (thickness/extent) is about 10^{-3} ! With a thickness of only 200 AU, the time scale for changing along the line of sight is only a few thousand years—within recorded human history! The ~ 10 -year time scale for variability of the Na optical absorption line against stars is satisfying confirmation of this rapid evolution (Meyer et al. 2012).

2.3 OH and HCO⁺: Tracers of Dark Molecular Gas

In Dark Molecular Gas, Hydrogen is molecular but the usual H₂ tracer, CO emission, is largely absent. CO requires protection from UV radiation, which occurs either from CO self-shielding or dust extinction. In these cases, H₂ is well-traced by OH (Lucas & Liszt 1996, Liszt & Lucas 2004) and also by HCO⁺ (Liszt & Pety 2012, Liszt et al. 2010), so much so that the observed column densities are linearly related:

$$\frac{N(OH)}{2N(H_2)} = 0.5 \times 10^{-7} \quad ; \quad \frac{N(HCO^+)}{2N(H_2)} = 1.2 \times 10^{-9} \quad (1)$$

and, of course, this means OH and HCO⁺ are also linearly related, with

$$\frac{N(HCO^+)}{N(OH)} = 0.03 \quad (2)$$

These linear relationships can be understood as the result of ion-molecule reactions arising in cool regions where Carbon is C⁺. The relevant reaction chain for OH production involves 7 rapid ion-

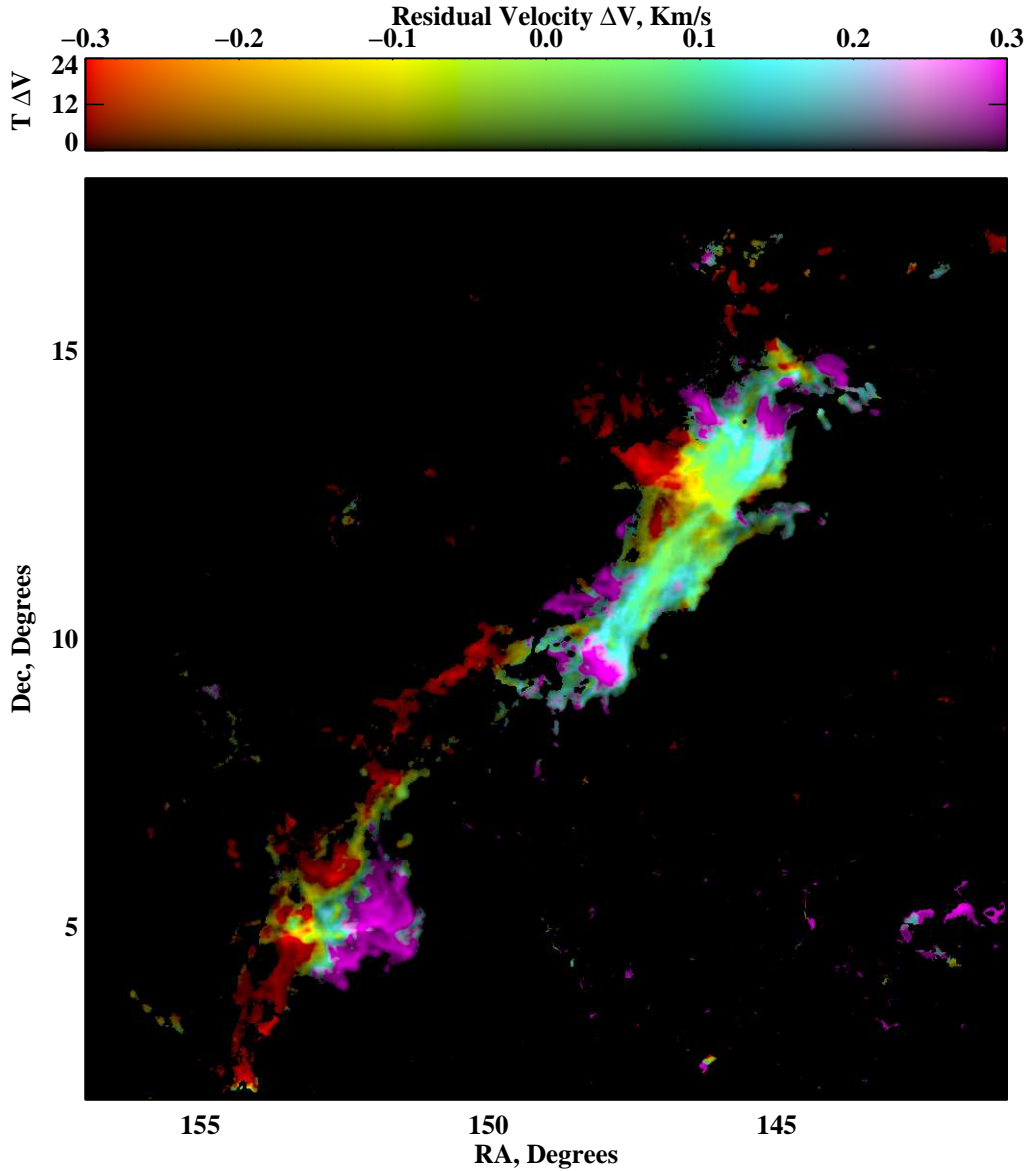
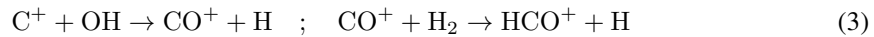


Fig. 1: Image of CNM (from GALFA data) in the Local Leo Cold Cloud (LLCC). Color indicates residual velocity (after subtracting a velocity gradient).

molecule reactions involving e^- , H, O, OH^+ , OH_2^+ , H_2 , H_2^+ , H_3^+ , and H_3O^+ (Wannier et al. 1993). Having formed OH, we obtain HCO^+ (Lucas & Liszt 1996):



The only problem with this scheme is that the ratio $N(HCO^+)/N(OH)$ is predicted to be about 20 times smaller than the observed ratio, which is a sad reflection on our understanding of astrochemistry. Nevertheless, the observed ratios for OH, HCO^+ , and H_2 in equations 1 and 2 are very robust, which is an empirical demonstration that OH and HCO^+ are excellent tracers of H_2 , particularly at low column densities where CO cannot survive.

2.3.1 The Millennium Survey's OH as a Tracer of Dark Molecular Gas

In the HT Millennium survey there was ‘extra’ spectrometer capability that allowed simultaneous observation of the two ‘main’ lines (1665 and 1667 MHz) of ground-state OH. The long integration times required for detecting HI Zeeman splitting provided excellent sensitivity for OH in absorption. Figure 2, which is based on those Millennium survey data, shows that OH traces Dark Molecular gas. Black stars show sources with detected OH absorption. Red circles show sources with detected CO emission¹ and green circles show no CO emission. Therefore, sources with both black stars and green circles have OH absorption but no CO emission, so these show Dark Molecular Gas. (Blue circles have no CO data).

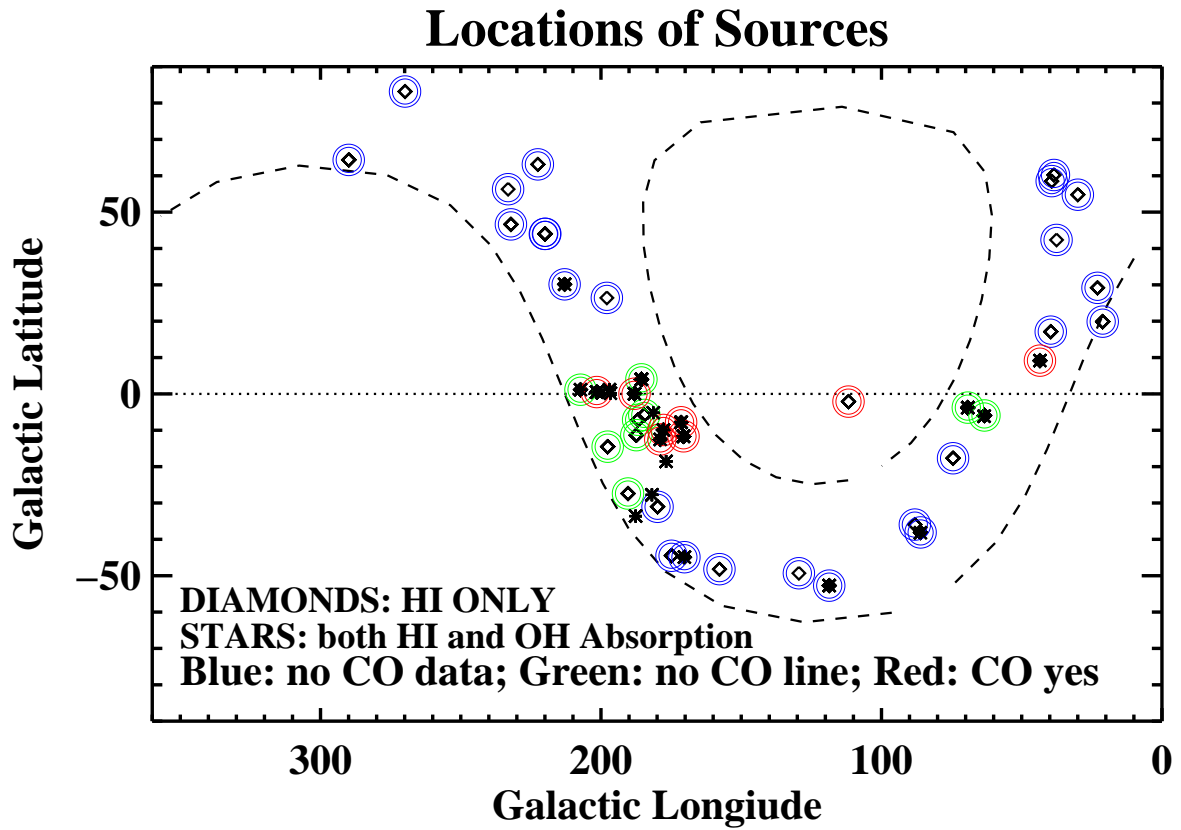


Fig. 2: Map of sources observed in the Millennium survey. Diamonds are sources showing HI absorption only. Stars show both HI and OH absorption. Blue circles show sources having no CO data. Green circles show sources having CO data, but no detected CO line. Red circles show sources having detected CO line.

There are eight sources with OH absorption but no CO emission. There are 7 sources showing both OH absorption and CO emission. Thus *Dark Molecular Gas (with no CO) is as common as Undark Molecular Gas (with CO)*. This result is consistent with Lucas & Liszt (1996), who observed 30 mm-wave continuum sources for absorption of HCO⁺ and of CO. HCO⁺ absorption lines are common, while CO absorption lines are uncommon.

¹ Here, we used CO emission data from Dame’s compilation (<http://www.cfa.harvard.edu/rtdc/CO/>). Other surveys are Liszt (1994) and Liszt & Wilson (1993), which we have not yet examined. However, for one source, 3C207, Dame found emission and Liszt (1994) did not. This demonstrates the need for better data!

2.3.2 OH as a Tracer: Absorption vs. Emission

Figure 3 exhibits as-yet unpublished histograms of the Millennium survey OH optical depths τ , emission line antenna temperature T_A , and excitation temperatures T_x . We decomposed all OH lines into Gaussian components and made histograms of the peaks. For the 1665 MHz line, the optical depths and antenna temperatures are multiplied by 9/5 so that the scales for the two lines are identical if the excitation is thermal. The histograms for the two lines do, indeed, look similar, so neither line is anomalously excited with respect to the other. This is reflected in the right panel of Figure 3, which shows the histogram of excitation temperatures for the Gaussian components. Typically, $T_x \sim 5$ K. The green histogram represents the background continuum brightness temperature T_C , which consists of the CBR plus the Galactic synchrotron background; typically, for these sources that lie away from the Galactic plane, $T_C \sim 3.5$ K.

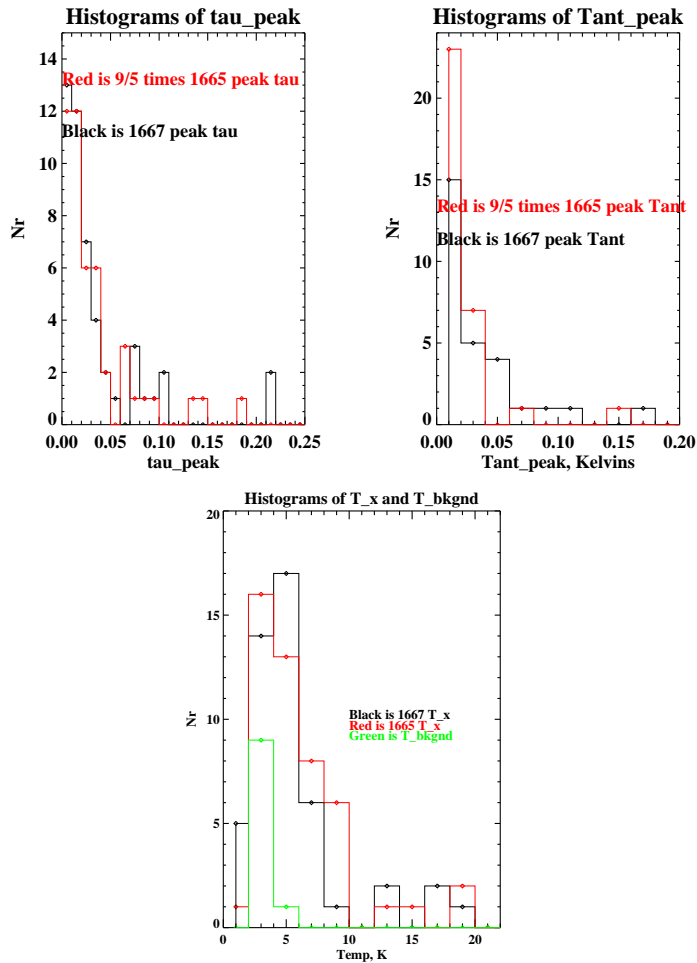


Fig. 3: Histograms of peak optical depth, antenna temperature in emission, and excitation temperature for the Gaussian components. Black shows 1667 MHz and red shows 9/5 times the peak optical depth for 1665 MHz.

The Millennium survey continuum sources generally have flux density $S \gtrsim 2$ Jy, so they produce continuum antenna temperatures in excess of about 20 K at Arecibo. For our weakest optical depths $\tau = 0.01$, the observed absorption line deflection is $\gtrsim 0.2$ K. In contrast, the OH emission lines are much weaker; nearly all the emission lines have deflections $\lesssim 0.1$ K. Thus, OH is much easier to detect in absorption than in emission. This is easy to understand when considering the excitation temperature.

For a frequency-switched emission spectrum of a single OH feature having peak optical depth τ seen against a continuum background brightness temperature T_C , the observed antenna temperature T_A is

$$\Delta T_A = [T_x - T_C] [1 - \exp(-\tau)] \quad (4)$$

Because $T_A \propto (T_x - T_C)$, the emission line intensities are significantly reduced.

3 GALACTIC EVOLUTION AND THE INTERSTELLAR MEDIUM

3.1 How Does Energy Flow in the Disk and Between the Disk and Halo?

The Milky Way is not a closed system. The evolution of the Milky Way is significantly impacted by the two-way flow of gas and energy between the Galactic disk, halo, and intergalactic medium. We have long known that the atomic hydrogen halo extends far beyond the disk of the Galaxy. In recent years we have come to realize that the halo is also a highly structured and dynamic component of the Galaxy. Although we can now detect hundreds of clumped clouds in the atomic medium of the halo (Ford et al. 2010), we are far from understanding the halo's origin and its interaction with the disk of the Galaxy.

It has been proposed that there may be two dominant sources of structure in the halo: one is the outflow of gas from the Galactic disk, and the second is the infall of gas from extragalactic space. The relative importance of these sources and their effects on the global evolution of the Milky Way are not known.

It seems that a significant fraction of the structure of gas in the Galactic halo may be attributed to the outflow of structures formed in the disk, but extending into the halo. An example of such a structure may be an HI supershell. There are several examples of HI supershells that have grown large enough to effectively outgrow the Galactic HI disk (e.g. McClure-Griffiths et al. 2003, McClure-Griffiths et al. 2006). When this happens, the rapidly decreasing density of the Galactic halo does not provide sufficient resistance to the shell's expansion and it will expand unimpeded into the Galactic halo, creating a chimney from disk to halo. These chimneys supply hot, metal-enriched gas to the Galactic halo and may act as a mechanism for spreading metals across the disk. It has been theorized that HI chimneys in the disk of the Galaxy may be a dominant source of structure for the halo through a Galactic Fountain model (Shapiro & Field 1976, Bregman 1980). Some Fountain models, e.g. de Avillez (2000), predict that cold cloudlets should develop out of the hot gas expelled by chimneys on timescales of tens of millions of years. Other Fountain theories, e.g. Mac Low et al. (1989), suggest that the cool caps of an HI supershell will extend to large heights above the Galactic plane before they break. Once broken, the remains of the shell caps could be an alternate source of small clouds for the lower halo.

Recent observational work has placed this theory on firmer footing, showing that the clumped clouds that populate the lower halo are not only more prevalent in regions of the Galaxy showing massive star formation than in less active regions, but that they extend higher into the halo in these regions (Ford et al. 2010). Now we would like to know how these clouds survive as cold, compact entities as they traverse the hot lower halo, with temperatures up to 10^5 K, and whether the cloud structures can tell us anything about their past journey through the halo.

Our ability to answer these questions is significantly hampered by our inability to image the detailed physical structure of the HI in the halo. With the present generation of all-sky surveys at $15'$ angular resolution and 1 km s^{-1} spectral resolution, it is not possible to explore the thermal and physical structure of these cloudlets, which may contain information about their origin, motion and evolution. Follow-up observations on several individual cloudlets show a tantalizing glimpse of possible head-tail structure and other evidence of interaction.

These observations may offer the opportunity to resolve a directional ambiguity with these clouds. In general we can measure only the absolute value of the z component of the cloud velocity with respect to the Galactic Plane, i.e. we cannot determine whether the clouds are moving towards or away from the Galactic Plane. Finding head-tail structure in the clouds can help resolve this ambiguity by showing the direction of motion. At present these follow-up observations are prohibitive, requiring hundreds of hours with interferometers to reach 100 mK at arcminute scales. The sensitivity and spectral resolution

of FAST will allow us to study the spatial and spectral structure of disk-halo clouds. We believe that the structure of the lower halo is related to the star formation rate in the disk below. FAST has greater sky coverage than Arecibo and extends into regions of the Galaxy where the star formation rate is of interest.

3.2 High Velocity HI Associated with the Milky Way and Magellanic System

Cosmological simulations predict that gas accretion onto galaxies is ongoing at $z = 0$. The fresh gas is expected to provide fuel for star formation in galaxy disks (Maller & Bullock 2004). In fact, galaxies like the Milky Way must have received fresh star formation fuel almost continuously since their formation in order to sustain their star formation rates. High velocity clouds (HVCs), first identified in HI 21 cm emission at anomalous (non-Galactic) velocities, have been suggested as a source of fuel (Quilis & Moore 2001). Some of the HI we see in the halo of the MW comes from satellite galaxies, some is former disk material that is raining back down as a galactic fountain, and some may be condensing from the hot halo gas (Putman 2006). The relative fractions of these structures are unknown. Furthermore, the detailed physics of how gas comes into the Milky Way disk is still unknown. How much gas flows into the disk through the halo, how fast does it flow, and what forces act on it along the way? Is the accretion of the Magellanic Stream a template for galaxy fuelling?

The Magellanic Stream provides the closest example of galaxy fuelling. The Magellanic Stream, which extends almost entirely around the Milky Way (Nidever et al. 2010), is gas stripped off the nearby Small Magellanic Cloud during its interaction with the Large Magellanic Cloud and the Milky Way. While the Magellanic Leading Arm is believed to be closely interacting with the Milky Way disk, the Northern tip of the Magellanic Stream is furthest from the Milky Way and contains a wealth of small scale structure (Stanimirović et al. 2008). By studying the details of the physical and thermal structure of the Magellanic Stream and its interaction with the Milky Way we will reveal its origin and evolution.

3.3 High and Intermediate Velocity Clouds in the Milky Way

High and intermediate velocity clouds (HVCs and IVCs) are believed to play important roles in both the formation and the evolution of the Galaxy. Some HVCs may be related to the Galactic Fountain; some are tidal debris connected to the Magellanic Stream (Putman et al. 2003, Stanimirović et al. 2008) or other satellites; some may be infalling intergalactic gas, and some may be associated with dark matter halos and be the remnants of the formation of the Local Group. The structure and distribution of high velocity gas probes tidal streams and the building blocks of galaxies providing critical information on the evolution of the Milky Way system. One problem that has long plagued HVC studies is the almost complete lack of distances to these objects, which has traditionally sparked debates about whether HVCs are Galactic or extragalactic. Although the distance problem is improving somewhat with increased number of distances using absorption towards halo stars, the problem remains. Regardless, the consensus now is that there are probably a variety of HVC origins.

The nearby HVCs can be used as probes of the thermal and density structure of the Galactic halo. HVCs have, in general, a high velocity relative to their ambient medium, which results in a ram pressure interaction between the cloud and medium. Recent HI observations have indeed shown that a significant fraction of the HVC population have head-tail or bow-shock structure (Brüns et al. 2000). By comparing the observed structures and thermal distributions within them to numerical simulations it is possible to determine basic physical parameters of the Galactic halo such as density, pressure, and temperature. In situations where the density and pressure of the ambient medium are known by independent methods the problem can be turned around to determine the distance to the observed clouds (Peek et al. 2007; Figure 4). Recent large-scale single dish surveys, the Galactic All-Sky Survey (GASS; McClure-Griffiths et al. 2009, Kalberla et al. 2010) and the HI-Galactic Arecibo L-Feed Array (GALFA; Peek et al. 2011b) have produced outstandingly detailed and sensitive images of HI associated with the Milky Way and Magellanic Stream. These surveys offer high spectral resolution, revealing how the spectral structure of

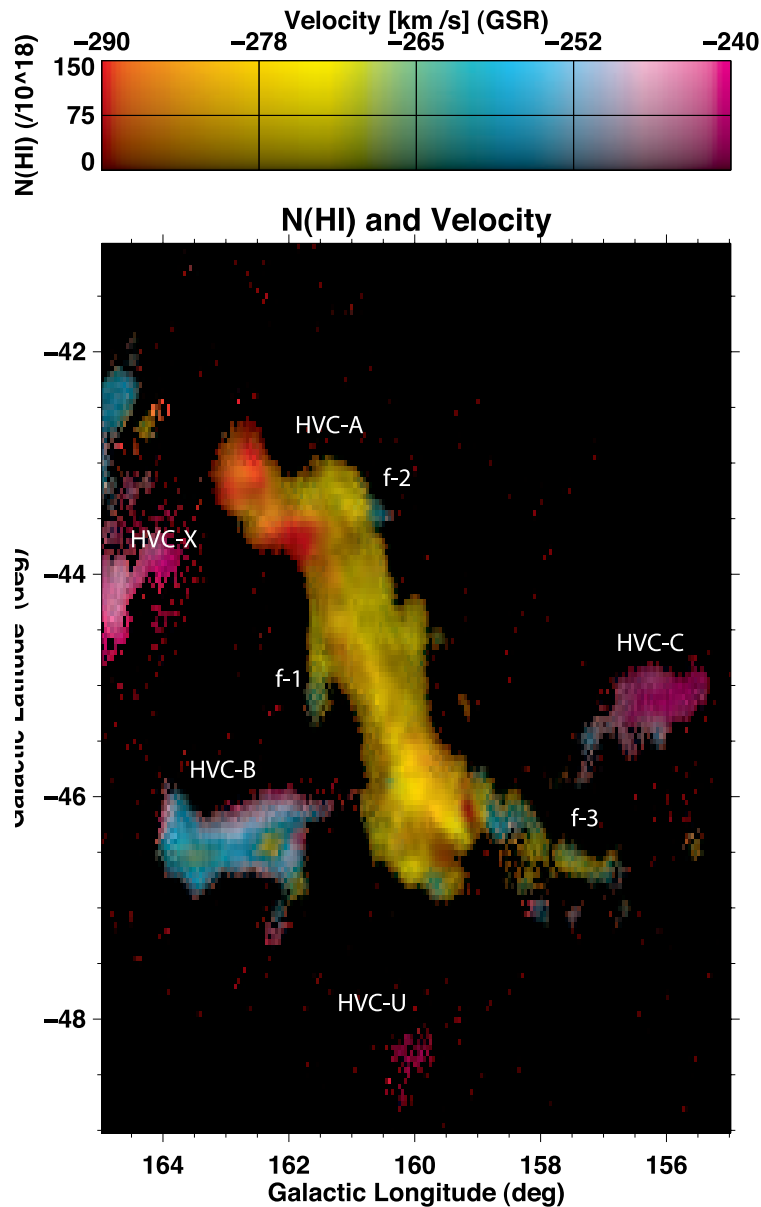


Fig. 4: The shards of [Peek et al. \(2007\)](#)'s HVC. HI column density (brightness) and central velocity (color).

disk-halo structures give important clues to their evolution. With these improvements we are beginning to resolve the structure of some of the mid-sized HVCs.

However, we do not yet have the sensitivity or resolution necessary to study the detailed physical and thermal structure over a large number of HVCs. It seems that the structure that we do see is just the tip of the iceberg. GASS is also revealing a wealth of tenuous filaments connecting HVCs to the Galactic Plane at column densities of $N(HI) \sim 10^{18} \text{ cm}^{-2}$. As an example, Complex L shows that the HVCs are interconnected by a thin, low column density filament and that this filament appears to extend to the Galactic disk. Filaments of HVCs such as these may be related to the cosmic web predicted in cosmological simulations. Observations of the M31-M33 system ([Braun & Thilker 2004](#), [Wolfe et al.](#)

2013) have revealed the local analogue of the cosmic web, showing that very low column density gas ($N(\text{HI}) \sim 10^{16} - 10^{17} \text{ cm}^{-2}$) connects the two galaxies.

4 THE ISM AT MODERATE TO HIGH REDSHIFT

We want to learn about galaxy evolution in the cosmological context, so we should pursue measurements at moderate to high redshift to the extent possible. Owing to sensitivity requirements, from a practical standpoint these are available in absorption, and in rare cases possibly in maser emission from OH, H₂O, or CH₃OH. Highly redshifted 21-cm HI absorption lines are seen in damped Ly α lines and also against the occasional radio-bright continuum source (Curran et al. 2011); in some of these cases, molecules also appear in absorption, especially OH (Chengalur et al. 1999). Studying such systems will provide limited, but unique, information on temperatures, chemical concentration, and magnetic field strengths—and how these quantities change with redshift.

5 THE ROLE OF FAST

5.1 Expand the GALFA Survey to an All-Sky FAST-HI Survey

We need to map the 21-cm line over the entire 22,000 deg² FAST sky—i.e., we need to do with FAST what GALFA did with Arecibo to obtain more sky coverage with the best combination of angular resolution and sensitivity. This will map the ISM morphology generally, including HVCs, and will enhance the sample of the unique structures discovered with GALFA: compact clouds and fibers. This survey should use the multibeam feed for observing efficiency and should cover at least GALFA’s velocity range ($\pm 800 \text{ km s}^{-1}$) and resolution (0.2 km s^{-1}). With a resolution of 2.9 arcmin and full sampling (pixel size $< 1.5 \text{ arcmin}$) and 12 seconds per pixel, the survey requires about 40000 hours with a single-pixel feed. With the 19-element feed in drift-scan mode, this is a 5000 hour project.

5.2 Expand the Millennium Survey: HI Zeeman Splitting with Simultaneous OH Emission/Absorption

Figure 5 says it all. The Millennium survey observed HI Zeeman splitting and OH absorption and it covered 76 sources, of which only 42 had detected magnetic fields. The statistical sample of measured Zeeman splittings is woefully small and desperately needs to be expanded. With FAST, a 0.5 Jy source has an antenna temperature roughly equal to the system temperature, so the continuum is strong and Zeeman sensitivity is high. There are 1072 such sources available to Fast, and ultimately each one should be included in a new Millennium survey.

Zeeman-splitting observations are time-consuming: typically tens of hours are required for each source. That works out to about 20,000 hours of telescope time; this survey will keep FAST occupied for a long time!

Surveying OH absorption is important for studying Dark Gas, and the OH lines are best studied in absorption. Even so, they are weak. Clearly, HI Zeeman-splitting and OH should be observed simultaneously because they have similar sensitivity requirements.

5.3 Map OH emission in well-chosen regions

Ultimately, understanding Dark Molecular Gas will require mapping of HI and also the DMG tracers. The two best DMG tracers are OH and HCO⁺; of these, OH has a much smaller critical density and is consequently a much better tracer in emission. FAST is the ideal telescope for this purpose. Mapping can begin with those fields already mapped in CO by Liszt & Pety (2012), and continue with other CO fields, including the peripheries of molecular clouds (e.g. Cotten & Magnani 2013, Allen et al. 2012).

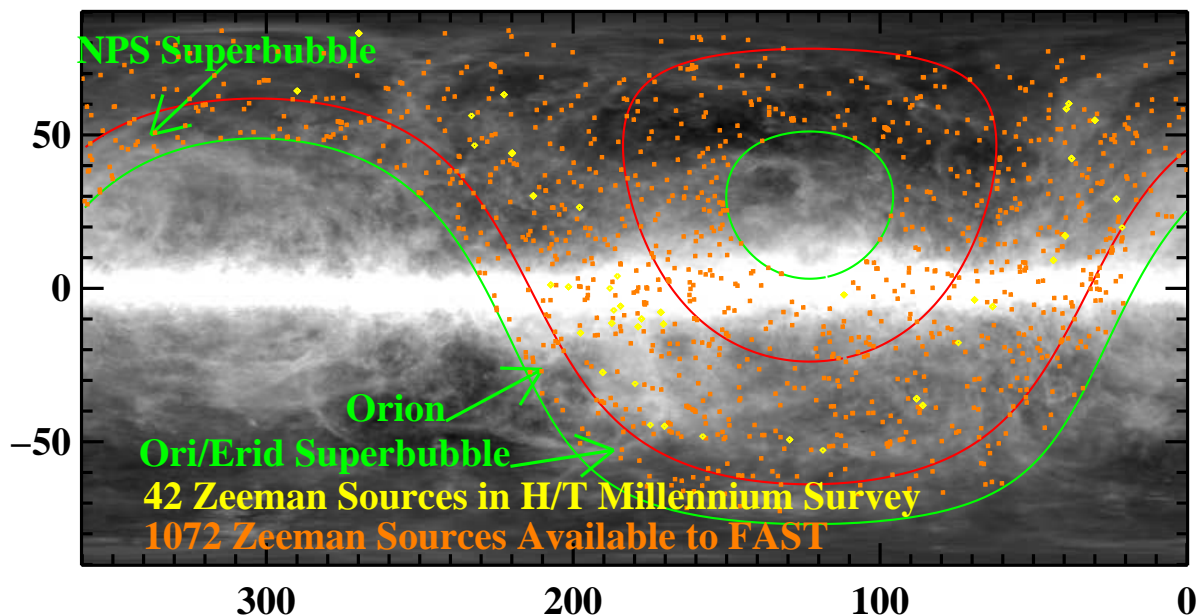


Fig. 5: Gray-scale image of the velocity-integrated HI emission for the whole sky. Red and green lines enclose the Arecibo sky and FAST coverage regions. Orange dots show all radio continuum sources with fluxes exceeding 0.5 Jy, which makes them suitable for measuring Zeeman splitting.

5.4 Moderate to High Redshift

DLAs and other cosmologically relevant lines, either HI in absorption or molecules—mainly OH—in absorption or maser emission, should be systematically observed as they are found.

The FAST’s large diameter, filled aperture, and sky coverage provide the angular resolution and sensitivity required to make it the best telescope for HI and OH emission maps. Together with Arecibo, FAST is uniquely suitable in providing the sensitivity required for the very weak OH lines in emission/absorption, and it will also do an excellent job for HI. The sky coverage will provide a greatly expanded set of interstellar structures, which is essential for obtaining a reliable statistical sample. The proposed novel commensal survey mode (Commensal Radio Astronomy FAST Survey – CRAFTS, Li et al. 2018a) will realize large-scale HI imaging simultaneously with pulsar search, making both types of surveys more efficient. We look forward to getting started!

Acknowledgements This work is supported by National Key R&D Program of China No. 2017YFA0402600, the CAS International Partnership Program No.114A11KYSB20160008, and NSFC No. 11725313.

References

- Allen, R. J., Hogg, D. E., & Engelke, P. D. 2015, *AJ*, 149, 123 [3](#)
 Allen, R. J., Ivette Rodríguez, M., Black, J. H., & Booth, R. S. 2012, *AJ*, 143, 97 [3](#), [11](#)
 Braun, R., & Thilker, D. A. 2004, *A&A*, 417, 421 [10](#)
 Bregman, J. N. 1980, *ApJ*, 236, 577 [8](#)
 Brüns, C., Kerp, J., Kalberla, P. M. W., & Mebold, U. 2000, *A&A*, 357, 120 [9](#)
 Chengalur, J. N., de Bruyn, A. G., & Narasimha, D. 1999, *A&A*, 343, L79 [11](#)
 Cotten, D. L., & Magnani, L. 2013, *MNRAS*, 436, 1152 [3](#), [11](#)
 Cotten, D. L., Magnani, L., Wennerstrom, E. A., Douglas, K. A., & Onello, J. S. 2012, *AJ*, 144, 163 [3](#)

- Curran, S. J., Whiting, M. T., Tanna, A., Bignell, C., & Webb, J. K. 2011, *MNRAS*, 413, L86 11
- de Avillez, M. A. 2000, *MNRAS*, 315, 479 8
- Dickey, J. M., Crovisier, J., & Kazès, I. 1981, *A&A*, 98, 271 2
- Ford, H. A., Lockman, F. J., & McClure-Griffiths, N. M. 2010, *ApJ*, 722, 367 8
- Grenier, I. A., Casandjian, J.-M., & Terrier, R. 2005, *Science*, 307, 1292 3
- Heiles, C., & Troland, T. H. 2003, *ApJ*, 586, 1067 2, 4
- Heiles, C., & Troland, T. H. 2005, *ApJ*, 624, 773 3
- Kalberla, P. M. W., McClure-Griffiths, N. M., Pisano, D. J., et al. 2010, *A&A*, 521, A17 9
- Komatsu, E., Dunkley, J., Nolta, M. R., et al. 2009, *ApJS*, 180, 330 1
- Li, D., Wang, P., Qian, L., et al. 2018a, *IEEE Microwave Magazine*, 19, 112 12
- Li, D., Tang, N., Nguyen, H., et al. 2018b, *ApJS*, 235, 1 2
- Liszt, H. 1994, *ApJ*, 429, 638 6
- Liszt, H., & Lucas, R. 1996, *A&A*, 314, 917 2
- Liszt, H., & Lucas, R. 2004, *A&A*, 428, 445 4
- Liszt, H. S., & Pety, J. 2012, *A&A*, 541, A58 3, 4, 11
- Liszt, H. S., Pety, J., & Lucas, R. 2010, *A&A*, 518, A45 4
- Liszt, H. S., & Wilson, R. W. 1993, *ApJ*, 403, 663 6
- Lucas, R., & Liszt, H. 1996, *A&A*, 307, 237 2, 4, 5, 6
- Mac Low, M.-M., McCray, R., & Norman, M. L. 1989, *ApJ*, 337, 141 8
- Maller, A. H., & Bullock, J. S. 2004, *MNRAS*, 355, 694 9
- McClure-Griffiths, N. M., Dickey, J. M., Gaensler, B. M., & Green, A. J. 2003, *ApJ*, 594, 833 8
- McClure-Griffiths, N. M., Ford, A., Pisano, D. J., et al. 2006, *ApJ*, 638, 196 8
- McClure-Griffiths, N. M., Pisano, D. J., Calabretta, M. R., et al. 2009, *ApJS*, 181, 398 9
- Meyer, D. M., Lauroesch, J. T., Peek, J. E. G., & Heiles, C. 2012, *ApJ*, 752, 119 4
- Nidever, D. L., Majewski, S. R., Butler Burton, W., & Nigra, L. 2010, *ApJ*, 723, 1618 9
- Peek, J. E. G., Heiles, C., Peek, K. M. G., Meyer, D. M., & Lauroesch, J. T. 2011a, *ApJ*, 735, 129 4
- Peek, J. E. G., Putman, M. E., McKee, C. F., Heiles, C., & Stanimirović, S. 2007, *ApJ*, 656, 907 9, 10
- Peek, J. E. G., Heiles, C., Douglas, K. A., et al. 2011b, *ApJS*, 194, 20 4, 9
- Putman, M. E. 2006, *ApJ*, 645, 1164 9
- Putman, M. E., Staveley-Smith, L., Freeman, K. C., Gibson, B. K., & Barnes, D. G. 2003, *ApJ*, 586, 170 9
- Quilis, V., & Moore, B. 2001, *ApJ*, 555, L95 9
- Remy, Q., Grenier, I. A., Marshall, D. J., & Casandjian, J. M. 2018, *A&A*, 611, A51 3
- Shapiro, P. R., & Field, G. B. 1976, *ApJ*, 205, 762 8
- Sommer-Larsen, J., Götz, M., & Portinari, L. 2003, *ApJ*, 596, 47 1
- Stanimirović, S., Hoffman, S., Heiles, C., et al. 2008, *ApJ*, 680, 276 9
- Wannier, P. G., Andersson, B.-G., Federman, S. R., et al. 1993, *ApJ*, 407, 163 5
- Wolfe, S. A., Pisano, D. J., Lockman, F. J., McGaugh, S. S., & Shaya, E. J. 2013, *Nature*, 497, 224 10
- Xu, D., & Li, D. 2016, *ApJ*, 833, 90 3
- Xu, D., Li, D., Yue, N., & Goldsmith, P. F. 2016, *ApJ*, 819, 22 3